J Mater Sci (2018) 53:7060–7071

Polymers

Synthesis and tribological properties of polyaniline functionalized by ionic liquids

Zhengfeng Cao[1] and Yanqiu Xia[1,2,*]

[1] School of Energy Power and Mechanical Engineering, North China Electric Power University, Beijing 102206, China
[2] State Key Laboratory of Solid Lubrication, Lanzhou Institute of Chemical Physics, Chinese Academy of Sciences, Lanzhou 730000, China

Received: 16 October 2017
Accepted: 11 January 2018
Published online: 18 January 2018

ABSTRACT

Two types of functionalized polyaniline (PAN) were synthesized based on the interfacial polymerization. PAN was characterized by scanning electron microscopy (SEM), energy-dispersive X-ray spectroscopy and Fourier transform infrared spectrometer. The results showed that synthesized PAN had different structures and was effectively modified by ionic liquids. The tribological properties of PAN as additives in polyethylene glycol (PEG) for steel/steel pairs were investigated in detail. The maximum reduction in friction and wear was achieved by PEG with addition of 0.2 wt% PAN. In particular, the wear volume was reduced by 3.8 times under 200 N. Moreover, the lubrication mechanisms were proposed by SEM and X-ray photoelectron spectroscopy (XPS) analysis of the worn surfaces.

Introduction

Friction is caused by relative motion or relative motion trend between two bodies in contact, and wear is the consequence of friction. Friction and wear consume a huge amount of energy and account for a lot of mechanical failures. Many aggressive efforts have been made to address the detrimental influence of friction and wear [1, 2]. Some research improves the tribological properties by dealing with the materials of friction pairs such as heat treatment, burnishing, turning, nitriding and plating [3–8]. Some other research explores new materials as lubricants or additives to meet the requirement of tribological performances [9–13]. These methods all achieve good results, and some of them have been successfully employed in industry, thereby saving energy and creating a considerable economic benefit.

Polyethylene glycol (PEG) has been widely utilized as high-performance lubricants, metal working fluids, gear oils, compressor lubricants and brake fluids in industry, as it is environmental friendly and degradable [11, 14]. However, PEG itself exhibits poor tribological performances under some harsh conditions [15]. Hence, it is necessary to employ friction reduction and anti-wear additives to improve the tribological properties of PEG during the actual applications. The development of suitable and high-performance additives has long been a research focus in the PEG-based lubricant field, and many lubricant

Address correspondence to E-mail: xiayq@ncepu.edu.cn

https://doi.org/10.1007/s10853-018-2028-7

additives have been evaluated to improve the tribological properties [11, 12, 14, 15].

Recently, polyaniline (PAN) as a lubricant additive has attracted our great interest because it exhibits good friction reduction and anti-wear abilities under multiple conditions [16]. However, in our previous work, due to the relatively large size and strong conjugated π electron system, micrometer PAN is easy to precipitate and agglomerate in lubricating oil, which result in limited tribological properties. Therefore, it is of great significance to fabricate nanometer PAN and improve its solubility. Some studies suggest that interfacial polymerization is a preferable approach to fabricate nanometer PAN. It involves that two reactive agents are dissolved, respectively, in two immiscible solvents and the polymerization reaction is taken place at the interface of two immiscible solvents [17]. To improve the solubility of PAN in solvents, many procedures have been adapted: (1) doping PAN by using functionalized protonic acids [18, 19]; (2) copolymerization or homopolymerization with aniline derivative [20]; (3) incorporation of polar functional groups [21]. According to the studies [22, 23], imidazolium-based ionic liquids (ILs) are sufficiently acidic in the 2-position and they have some favorable π–π interactions and hydrogen bonding interactions with PAN. Therefore, imidazolium-based ILs may be utilized as functionalized protonic acids to dope PAN and donate functional groups which can be incorporated onto PAN via π–π interactions and hydrogen bonding interactions. These previous studies provide a rich theoretical and experimental support to prepare nanometer PAN with improved solubility. Thus, PAN may hold a great promise as an ideal material for a huge range of applications.

Herein, two types of functionalized PAN were synthesized on the basis of interfacial polymerization. The structures and functionalization of obtained PAN were characterized and analyzed by scanning electron microscopy (SEM), energy-dispersive X-ray spectroscopy (EDS) and Fourier transform infrared spectrometer (FT-IR). The tribological properties of PAN as additives in PEG for steel/steel contacts were investigated under different conditions in detail. After friction and wear test, the morphologies and chemical compositions of the worn surfaces were observed and analyzed by SEM and X-ray photoelectron spectroscopy (XPS), respectively. Finally, the reasonable lubrication mechanisms of the functionalized PAN were also proposed.

Experimental details

Materials

Polyethylene glycol (PEG400), aniline, ammonium persulfate (APS) and acetone were all purchased from Sinopharm Chemical Reagent Co., Ltd, and they are all of analytical reagent grade. 1-butyl-3-methylimidazolium hexafluorophosphate ([Bmim][PF_6], $>99\%$) and 1-hexyl-3-methylimidazolium hexafluorophosphate ([Hmim][PF_6], $>99\%$) were obtained from J&K Scientific Ltd.

Preparation and characterization of functionalized PAN

The functionalized PAN was synthesized by the following steps. First, 10 g of distilled water containing 0.98 g APS and 10 g of ILs containing 0.4 g aniline were efficiently dispersed for 10 min by ultrasonic wave, respectively. Second, the two solutions were slowly transferred into a breaker, and then, an interface was formed between distilled water and ILs. After 10 min, green PAN was generated at the interface of water and ILs. With no disturbance, the reaction was continuous for 24 h at room temperature. Finally, the solution was filtered and washed with acetone and distilled water for several times, and then, filtrate cakes were dried using a heat oven at 40 °C for 12 h to obtain the functionalized PAN (which were abbreviated as PAN-[Bmim][PF_6] and PAN-[Hmim][PF_6]).

The structures of the PAN-[Bmim][PF_6] and PAN-[Hmim][PF_6] were characterized by a SU8010 scanning electron microscopy (SEM, Hitachi). The Fourier transform infrared spectra (FT-IR) of ILs and PAN were recorded using a FT-IR spectrometer (Thermo Fisher Scientific) in the wavenumber range of 4000–400 cm^{-1}. The chemical compositions of functionalized PAN were detected by an EVO-18 scanning electron microscopy–energy-dispersive X-ray spectroscopy (SEM–EDS) (Zeiss SEM, Bruker EDS) with 7.5 nm beam current under 12 kv accelerating voltage.

Preparation and tribological tests of lubricants

The obtained PAN-[Bmim][PF_6] and PAN-[Hmim][PF_6]) were dispersed in PEG via vigorous stirring for 30 min to prepare homogeneous solutions as the to-be-tested lubricants, respectively. The concentration of samples in PEG was adjusted as 0.1, 0.2, 0.3 and 0.4% (mass fraction, the same hereafter). The ILs including [Bmim][PF_6], [Hmim][PF_6] were also added into PEG to prepare lubricants in the manner as just described.

The tribological performances of lubricants for steel/steel pairs were investigated on a MFT-R4000 reciprocal friction tester with a ball-on-block configuration, which was produced by State Key Laboratory of Solid Lubrication, Lanzhou Institute of Chemical Physics, Chinese Academy of Sciences (Lanzhou, China). The upper ball (AISI 52100 steel ball, diameter 5 mm, hardness 710 Hv) was driven to slide reciprocally against the lower block (Ø24 mm × 7.9 mm, AISI 52100 steel, hardness 590 Hv, surface roughness 0.05 um) at a stroke of 5 mm, a frequency of 5 Hz and a normal load of 50–200 N (corresponding to the Hertzian pressure in the range of 1.7–2.7 GPa) for a duration of 30 min at room temperature (RT). Before and after each friction test, the steel balls and lower blocks were cleansed in acetone for 10 min utilizing an ultrasonic cleaner. Prior to test, about 0.5 g lubricant was added to the friction region and every test was conducted thrice to get more responsible values. A computer noted down the coefficient of friction, and a Micro-XAM 3D surface mapping microscopy profile meter determined the wear volumes on the steel blocks.

The tribological properties of lubricants at high temperature were evaluated on a MS-10J four-ball test machine (Xiamen Tenkey Automation Co., Ltd, Xiamen, China). The test parameters were set at a rotating speed of 1450 rpm and a load of 392 N for 30 min under the temperature of 120 °C. The test balls are made of GCr 15 bearing steel (diameter 12.7 mm, hardness 650–700 Hv). A computer and an optical microscopy equipped on the four-ball tester were employed to determine the coefficient of friction and wear widths of the three stationary balls, respectively.

Surface analysis

After friction and wear test, the lower blocks were ultrasonically cleansed in acetone for 10 min. An EVO-18 SEM (Zeiss, Germany) was employed to take the images of the wear scars and a PHI-5702 multifunctional X-ray photoelectron spectroscopy (XPS, American Institute of Physics Electronics Company) with K-alpha irradiation as the excitation source was employed to analyze the chemical states of the characteristics elements on the rubbing surfaces. A pass energy of 29.3 eV characterized the binding energies of the target elements with the binding energy of carbon (C1s 284.6 eV) as the reference.

Results and discussion

Analysis of functionalized PAN

The SEM morphologies of the PAN-[Bmim][PF_6] and PAN-[Hmim][PF_6] are provided in Fig. 1. It is clearly visible that two types of PAN present different structures, where PAN-[Bmim][PF_6] is rod-shaped with the diameter of about 100 nm and PAN-[Hmim][PF_6] shows spherical shape with the diameter of about 120 nm. Interfacial polymerization synthesizes the product based on interface nucleation mechanism, and the interactions between the solvent and aniline molecules have an important effect on the movement speed of the aniline to the reaction interface [24]. In general, a relatively fast movement speed is favorable for the formation of rod-shaped PAN [25]. The viscosities of [Bmim][PF_6] and [Hmim][PF_6] are 366 and 586 cP, respectively, and it is well known that a lower viscosity leads to a better fluidity. Therefore, the aniline molecules dissolved in [Bmim][PF_6] could move faster toward the reaction interface, resulting in that two types of PAN possess different shapes.

FT-IR was employed to characterize the functional groups of ILs and PAN. As shown in Fig. 2a, the characteristic peak at 839 cm^{-1} belongs to the P–F stretching vibration of anions and the characteristic peak at 1562 cm^{-1} belongs to the C=N stretching vibration of the imidazolium ring [23, 26]. The peaks located at 3162 and 2968 cm^{-1} are assigned to the H–C–C–H asymmetric stretching vibration of imidazolium ring and C–H stretching vibration of alkyl chains, respectively [27]. As shown in Fig. 2b, PAN

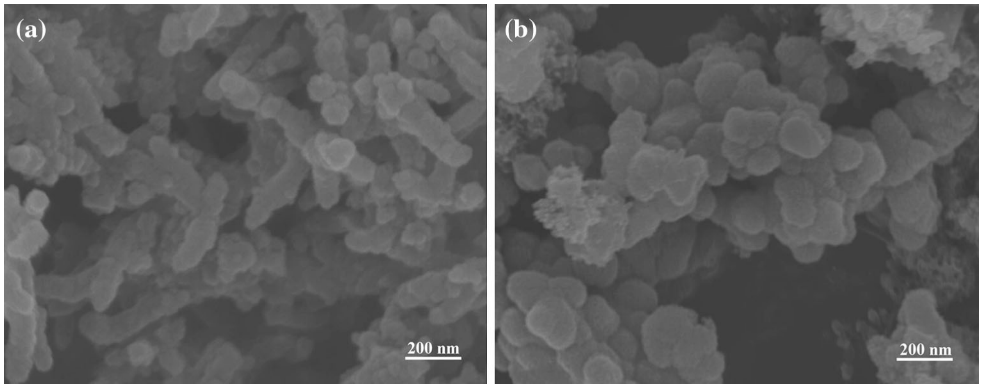

Figure 1 SEM morphologies of **a** PAN-[Bmim][PF_6] and **b** PAN-[Hmim][PF_6].

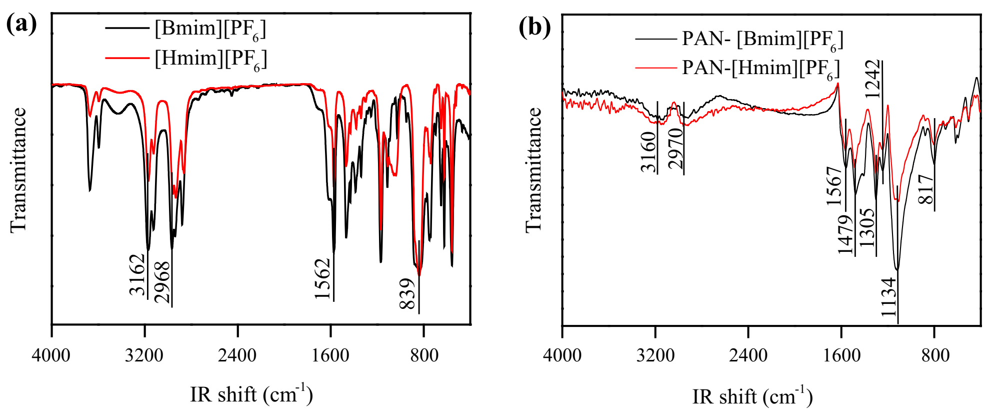

Figure 2 FT-IR spectra of ILs and functionalized PAN.

has the characteristic peaks of quinonediimine ring and benzene ring vibration at 1567 and 1479 cm^{-1}, respectively. The peaks at 1305 and 1242 cm^{-1} are assigned to the C–N stretching vibrations of secondary aromatic amine, and the peaks at 1134 and 817 cm^{-1} are assigned to the C–H bending vibration of benzene ring [23, 27]. FT-IR was employed to confirm the presence of functional groups from ILs on the PAN. However, as shown in the low wavenumber range (400–2000 cm^{-1}) of FT-IR spectra, the presence of functional groups of ILs could neither be confirmed nor excluded because the peaks of ILs are almost overlapped by the peaks of PAN. Fortunately, the FT-IR spectra recorded in the region above 2500 cm^{-1} are more favorable to detect the functional groups. The peaks at 3160 and 2970 cm^{-1} belong to the H–C–C–H asymmetric stretching vibrations of imidazolium ring and C–H stretching of alkyl chains from ILs, respectively [23]. The results suggest that PAN has been successfully modified with imidazolium-based ILs via π–π interactions and hydrogen bonding interactions.

SEM–EDS as a powerful facility can effectively characterize the chemical compositions and distribution, so it was employed to further confirm the presence of functional groups on PAN. Figure 3 displays the EDS elemental surface distribution images of the PAN-[Bmim][PF_6] and PAN-[Hmim][PF_6]. It is clearly visible that the characteristics elements of imidazolium-based ILs have reached high-density coverage on PAN, which gives a direct evidence for the successful modification of PAN via π–π interactions and hydrogen bonding interactions.

The unique functions of imidazolium-based ILs in the polymerization

Two types of PAN were successfully synthesized based on interfacial polymerization at the interface between [Bmim][PF_6]/[Hmim][PF_6] and water. The FT-IR and SEM–EDS analysis demonstrates that PAN was effectively modified with imidazolium-based ILs during the polymerization. Herein, the unique functions of the imidazolium-based ILs can be

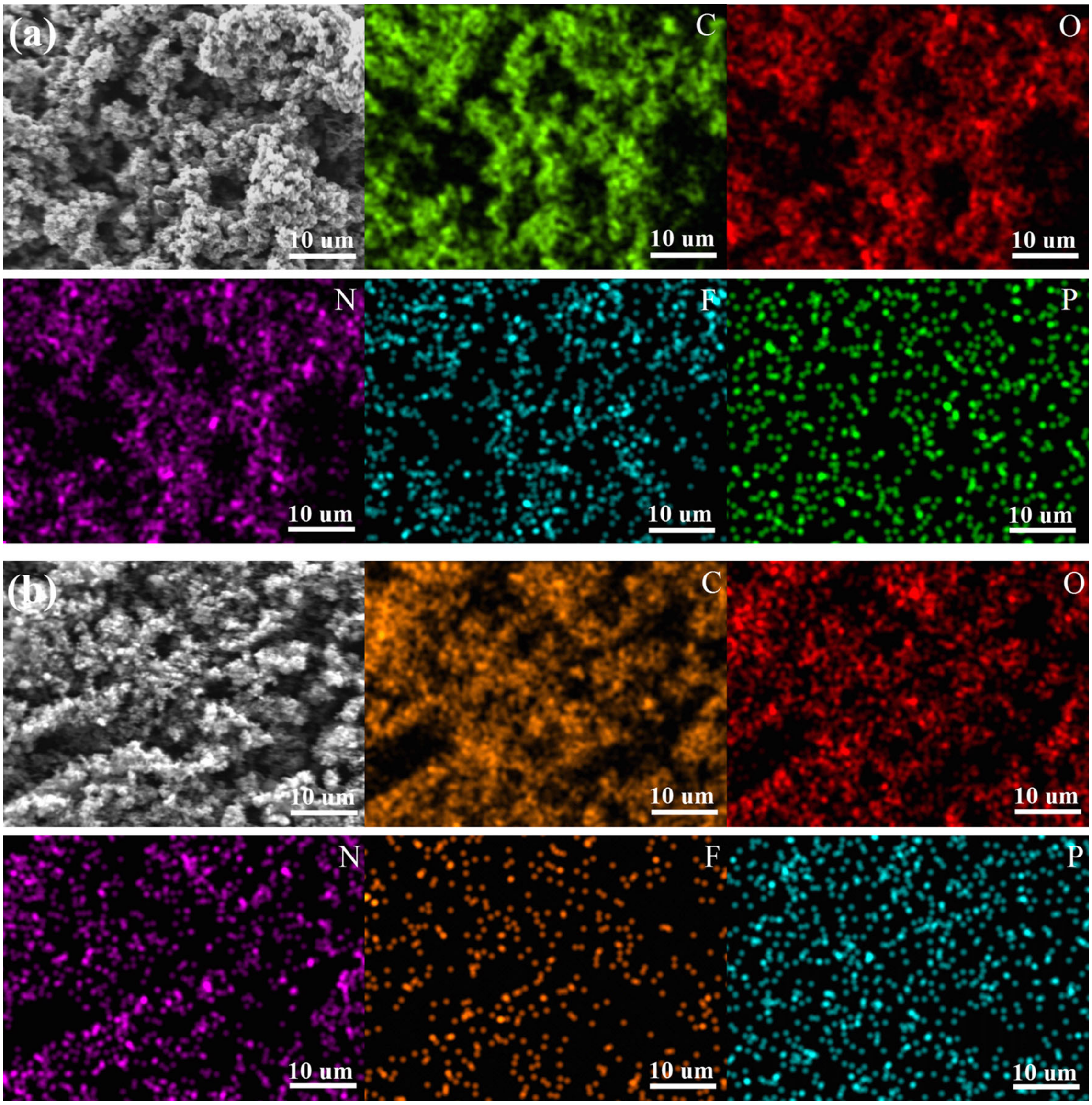

Figure 3 EDS elemental surface distribution images of **a** PAN-[Bmim][PF_6] and **b** PAN-[Hmim][PF_6].

summarized by the following aspects: (1) ILs serve as liquid phase to dissolve the aniline monomers for the polymerization of PAN. (2) ILs serve as functionalized acids to provide protons to dope PAN during the polymerization. This synthetic method also eliminates the usage of extra protonic acids as dopant. (3) ILs provide functional groups which can be incorporated onto PAN via π-π interactions and hydrogen bonding interactions, resulting in preferable solubility and tribological properties.

Tribological properties of functionalized PAN as the additives in PEG

An optimal concentration of solid lubricant additive has a significant improvement on the tribological properties. Figure 4 shows the average coefficient of friction and wear volumes as a function of the additive concentrations in PEG at 50 N, 5 Hz and RT. As shown in Fig. 4a, b, the overall trends of coefficient of friction and wear volumes decrease first and then increase with the increasing additive concentrations. The preferable improvement on friction reduction and anti-wear abilities is obtained by the PEG with the addition of 0.2% additives. Figure 4c, d compares

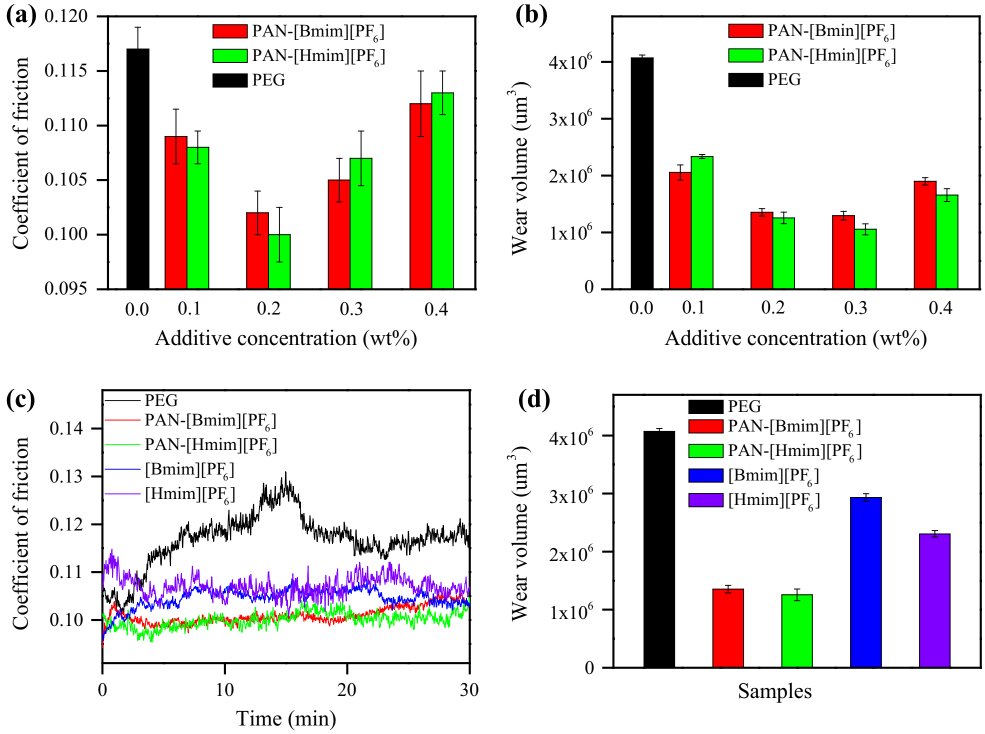

Figure 4 Average coefficient of friction **a** and wear volumes **b** for PEG plus PAN-[Bmim][PF_6] or PAN-[Hmim][PF_6] at different concentrations, coefficient of friction **c** and wear volumes **d** for PEG and PEG plus 0.2% different additives at 50 N, 5 Hz and RT.

the tribological properties of PEG in the absence and presence of 0.2% different additives. It is visible that PAN-[Bmim][PF_6] and PAN-[Hmim][PF_6] exhibit lower and more stable coefficient of friction than others, and their wear volumes are also reduced by about three times as compared to pure PEG. This reveals that PEG containing 0.2% functionalized PAN could have preferable friction reduction and anti-wear abilities.

Figure 5 presents the average coefficient of friction and wear volumes of PEG plus 0.2% different additives at multiple loads, 5 Hz and RT. Compared with PEG, [Bmim][PF_6] and [Hmim][PF_6], two types of functionalized PAN all exhibit lower coefficient of friction and wear volumes as the load increases from 50 to 200 N. At the high load of 200 N, the addition of PAN-[Bmim][PF_6] and PAN-[Hmim][PF_6] can reduce the wear volumes by 3.8 and 2.4 times as compared to pure PEG. This is attributed to the superior anti-wear ability of PAN-[Bmim][PF_6] and PAN-[Hmim][PF_6] because the functionalized PAN could prevent the direct contact between the friction interfaces and an

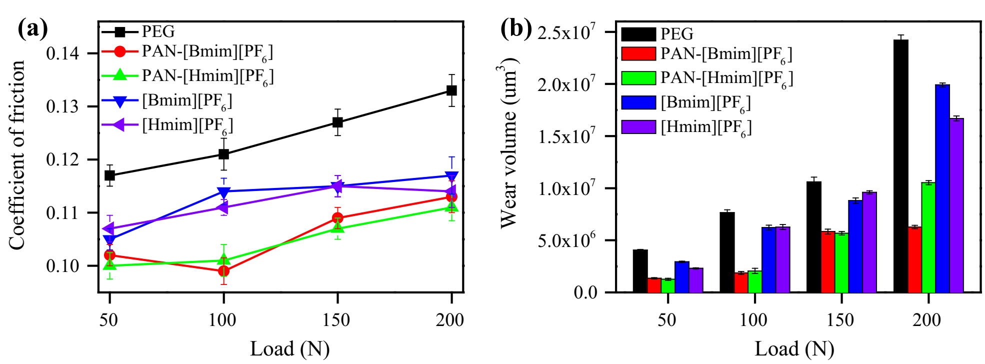

Figure 5 Average coefficient of friction **a** and wear volumes **b** for PEG and PEG plus 0.2% different additives at multiple loads, 5 Hz and RT.

effective tribofilm is generated on the rubbing surfaces by physical adsorption and tribochemical reaction throughout the sliding process.

A MS-10J four-ball tester is also employed to investigate the tribological properties of different lubricants at 120 °C and 392 N, and the results are depicted in Fig. 6. It is visible that four types of additives all can effectively lower the coefficient of friction and wear widths. During the first 10 min of friction test, all the lubricants have running-in period with fluctuant coefficient of friction. As time goes on, the friction coefficient of PAN-[Bmim][PF_6] and PAN-[Hmim][PF_6] gradually decreases, whereas [Bmim][PF_6] and [Hmim][PF_6] exhibit larger coefficient of friction than before. Figure 6b also indicates two types of functionalized PAN have preferable anti-wear ability in PEG. Compared with pure PEG, the biggest reduction in wear width is obtained by PEG with addition of 0.2% PAN-[Hmim][PF_6] which reduces the wear width by 41%. These results demonstrate that PAN-[Bmim][PF_6] and PAN-[Hmim][PF_6] are capable of forming an effective boundary lubricating film to improve the friction reduction and anti-wear abilities at 120 °C.

SEM and XPS analysis of the worn surfaces

Figure 7 shows the SEM morphologies of worn surfaces on the steel disks in the absence and presence of 0.2% each of the different additives at 200 N, 5 Hz and RT. As shown in Fig. 7a and b, the worn surfaces lubricated by PEG acquire considerably wider and deeper wear scar. There are a number of deep and narrow furrows which imply severe wear taken place in this situation. As shown in Fig. 7c–f, the addition of PAN-[Bmim][PF_6] and PAN-[Hmim][PF_6] in PEG not only reduces the wear widths, but also makes the worn surfaces smoother, indicating that functionalized PAN has a preferable anti-wear ability. In the case of the PEG containing [Bmim][PF_6] and [Hmim][PF_6], although the wear widths and worn surfaces are improved to some extent, some deep grooves and corrosion points appear on the worn surfaces. Furthermore, it can be also found that the worn surfaces lubricated by PAN-[Bmim][PF_6] and PAN-[Hmim][PF_6] have no corrosion points, which demonstrates that PAN-[Bmim][PF_6] and PAN-[Hmim][PF_6] could reduce the corrosion to enhance the tribological properties during the friction process. Based on the SEM analysis, the anti-wear ability of different lubricants can be arranged as follows: PAN-[Bmim][PF_6] > PAN-[Hmim][PF_6] > [Hmim][PF_6] > [Bmim][PF_6] > PEG. This is also in accordance with previous results shown in Fig. 5, which proves that PAN-[Bmim][PF_6] and PAN-[Hmim][PF_6] as the additives in PEG can remarkably enhance the anti-wear ability.

Functionalized PAN was presented as the lubricant additives to enhance the tribological properties for PEG and the preferable friction reduction, and anti-wear abilities have been proved in this work. To probe the lubrication mechanisms of functionalized PAN, XPS was employed to characterize the chemical states of typical elements on the rubbing surfaces lubricated by different functionalized PAN. As shown in Fig. 8, it is visible that the Fe, O, F, N and P on the rubbing surfaces have similar binding energies, indicating that they experienced similar tribochemical reaction during the sliding process. The spectrum of Fe2p exhibits peaks at about 724.3 and 710.8 eV, which may correspond to Fe_2O_3 and Fe_3O_4 [28, 29]. The peaks of O1s located at 530.0–531.5 eV

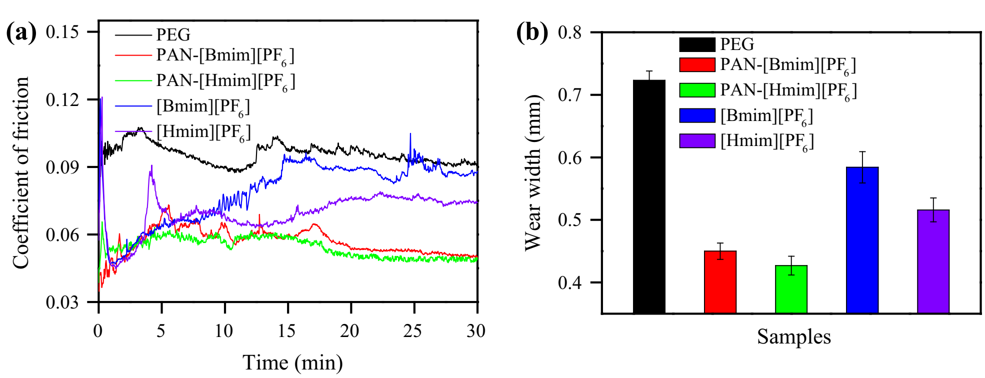

Figure 6 Coefficient of friction as a function of time **a** and wear width **b** for PEG and PEG plus different additives (0.2%) at 120 °C, 392 N in four-ball tests.

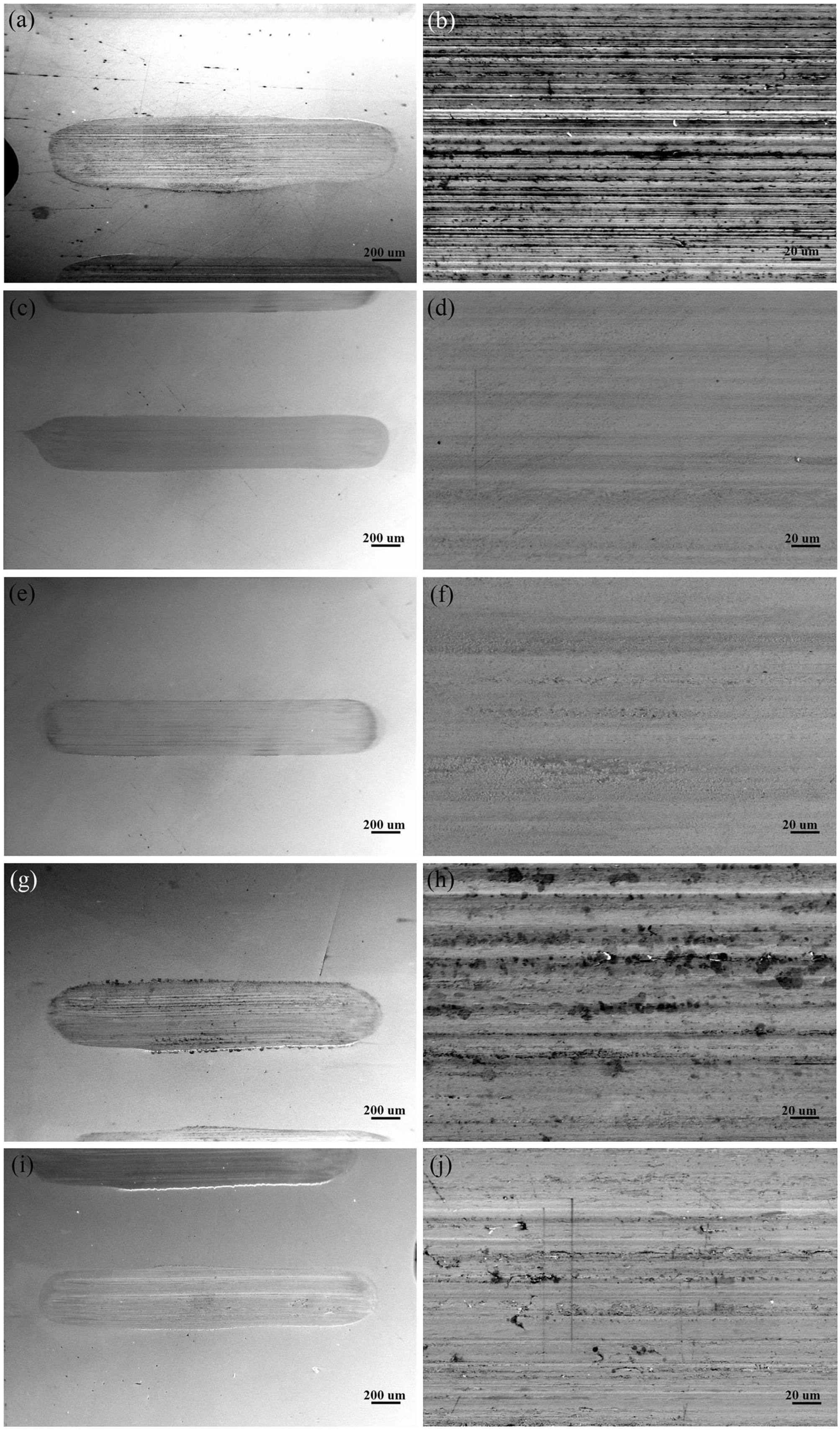
(a)
200 um
(b)
20 um
(c)
200 um
(d)
20 um
(e)
200 um
(f)
20 um
(g)
200 um
(h)
20 um
(i)
200 um
(j)
20 um

◀**Figure 7** SEM morphologies of worn surfaces on steel disks lubricated by **a** and **b** PEG, **c** and **d** PAN-[Bmim][PF_6], **e** and **f** PAN-[Hmim][PF_6], **g** and **h** [Bmim][PF_6], **i** and **j** [Hmim][PF_6] at 200 N, 5 Hz and RT.

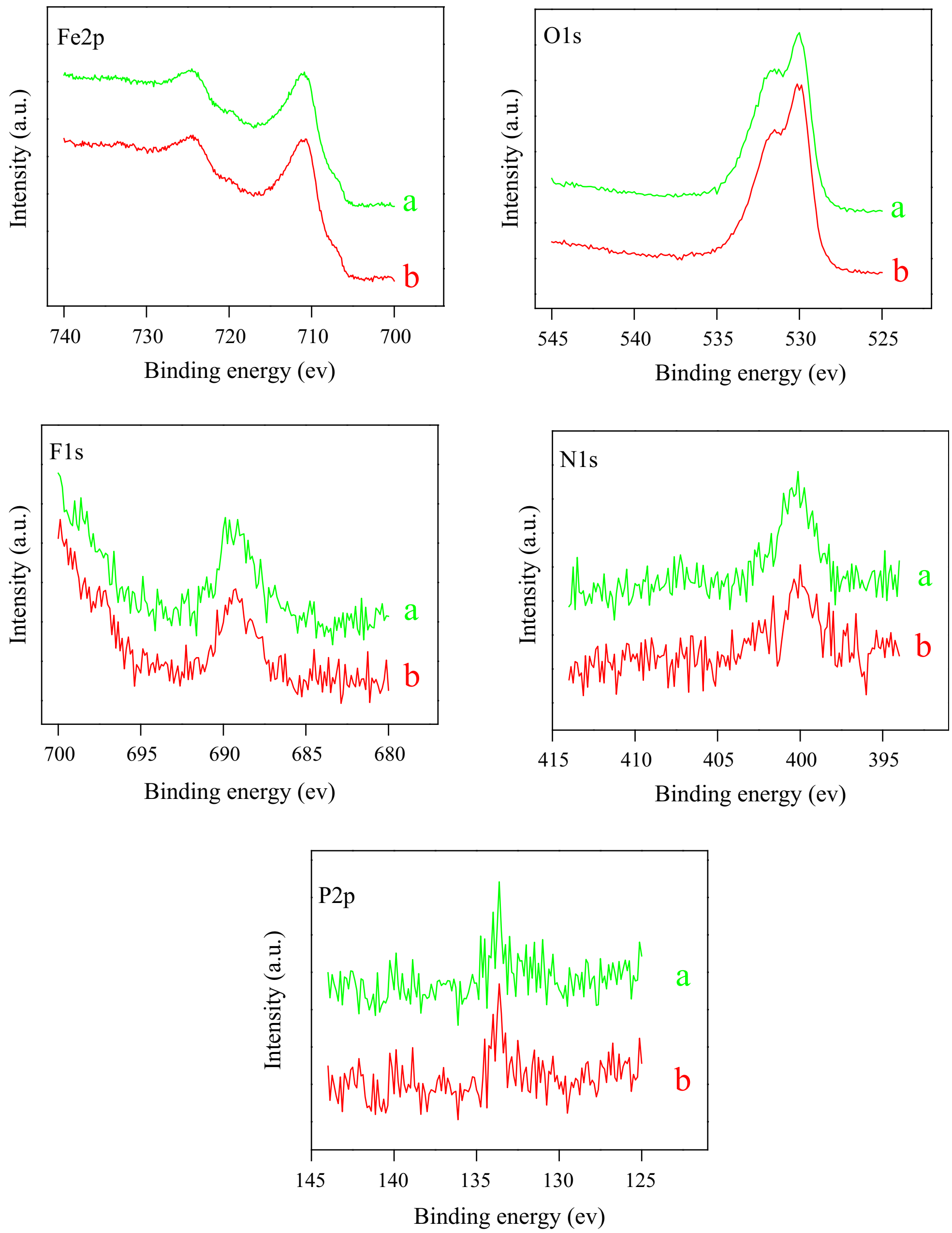

Figure 8 XPS spectra (Fe2p, O1s, F1s, N1s and P2p) of the worn surfaces lubricated by **a** PEG + 0.2 wt% PAN-[Bmim][PF_6] and **b** PEG + 0.2% [Hmim][PF_6].

may be assigned to FeO and C–O compounds, indicating the generation of complex oxide species [30]. The peaks at about 684.5 and 689.0 eV on the spectrum of F1 s may correspond to FeF_2, FeF_3 and C–F binding [28, 30]. The spectrum of N1s has a wide peak centered at 400.2 eV, which may belong to the nitrogen atoms in the imidazolium ring [12, 30, 31]. It may be an evidence for the physical adsorption of functionalized PAN on the rubbing surfaces. The peak of P2p at 133.5 eV suggests the existence of $FePO_4$ [30–32]. XPS analysis reveals that two types of functionalized PAN as additives in PEG not only generate a protective film which is composed of FeO,

Fe_2O_3, Fe_3O_4, FeF_2, FeF_3 or $FePO_4$ by complex tribochemical reactions, but also form a physical adsorption film to enhance the friction reduction and anti-wear abilities.

In addition, it is well known that nanoparticles such as carbon nanotubes, Cu, SiO_2 and TiO_2 can achieve the rolling effect by acting as bearings between the friction interfaces, thereby reducing the shear force to enhance the tribological properties [33–35]. As shown in Fig. 1, because the structures of functionalized PAN are similar to the particles, they may perform the rolling effect as well. During the friction process, the functionalized PAN also can exhibit a mending effect by filling the wear scratches, thereby reducing the surface roughness to improve the tribological properties [14, 34–37]. Meanwhile, particles modified with functional ILs could have superior stability in lubricants and easily adsorb on the worn surfaces to form a protective film [26]. Consequently, based on the characterization and analysis of functionalized PAN, and the SEM and XPS analysis of the worn surfaces, the preferable friction reduction and anti-wear abilities of functionalized PAN mainly depend on the synergistic lubricating effect including rolling and mending effects and the physical adsorption and the tribochemical reaction film on the worn surfaces. Hence, the functionalized PAN could hold a great potential as lubricant additives for a wide range of applications.

Conclusions

The functionalized PAN including PAN-[Bmim][PF_6] and PAN-[Hmim][PF_6] has been successfully synthesized at the interface of ILs and water based on the interfacial polymerization. SEM analysis of PAN shows that PAN-[Bmin][PF_6] is rod shape and the PAN-[Hmim][PF_6] is spherical shape. This is attributed to the different viscosities of ILs and the π–π and hydrogen bonding interactions between PAN and ILs. The FT-IR and EDS analysis demonstrates that PAN was effectively functionalized by imidazolium-based ILs. Tribological results indicate that PEG containing 0.2 wt% functionalized PAN exhibits the minimum coefficients of friction and wear volumes for steel/steel pairs under different conditions. SEM morphologies and XPS spectra of the worn surfaces suggest that the preferable friction reduction and anti-wear abilities of functionalized PAN were attributed to the synergistic lubricating effect including rolling and mending effects and the physical adsorption and the tribochemical reaction film on the worn surfaces. Therefore, taking into account the simple and effective synthetic method and preferable tribological properties, functionalized polyaniline in association with ILs can serve as lubricant additives for a range of applications.

Acknowledgements

This work is supported by the National Natural Science Foundation of China (Grant 51575181) and Beijing Municipal Natural Science Foundation (Grant 2172053).

Compliance with ethical standards

Conflict of interest The authors declare that they have no conflict of interest.

References

[1] Holmberg K, Andersson P, Erdemir A (2012) Global energy consumption due to friction in passenger cars. Tribol Int 47:221–234

[2] Rapoport L, Fleischer N, Tenne R (2003) Fullerene-like WS_2 nanoparticles: superior lubricants for harsh conditions. Adv Mater 15:651–655

[3] Hassani FZ, Ketabchi M, Bruschi S, Ghiotti A (2016) Effects of carbide precipitation on the microstructural and tribological properties of Co–Cr–Mo–C medical implants after thermal treatment. J Mater Sci 51:4495–4508. https://doi.org/10.1007/s10853-016-9762-5

[4] Määttä A, Vuoristo P, Mäntylä T (2001) Friction and adhesion of stainless steel strip against tool steels in unlubricated sliding with high contact load. Tribol Int 34:779–786

[5] Bourithis L, Papadimitriou GD, Sideris J (2006) Comparison of wear properties of tool steels AISI D2 and O1 with the same hardness. Tribol Int 39:479–489

[6] Tobola D, Brostow W, Czechowski K, Rusek P, Wronska I (2015) Structure and properties of burnished and nitrided AISI D2 tool steel. Mater Sci 21:511–516

[7] Tobola D, Brostow W, Czechowski K, Rusek P (2017) Improvement of wear resistance of some cold working tool steels. Wear 382–383:29–39

[8] Zhou SX, Wu LM, Shen WD, Gu GX (2004) Study on the morphology and tribological properties of acrylic based

polyurethane/fumed silica composite coatings. J Mater Sci 39:1593–1600. https://doi.org/10.1023/B:JMSC.0000016157.19241.57
[9] Scharf TW, Prasad SV (2013) Solid lubricants: a review. J Mater Sci 48:511–531. https://doi.org/10.1007/s10853-012-7038-2
[10] Cao ZF, Xia YQ (2017) Study on the preparation and tribological properties of fly ash as lubricant additive for steel/steel pair. Tribol Lett 65:104. https://doi.org/10.1007/s11249-017-0885-x
[11] Ghaednia H, Hossain MS, Jackson RL (2016) Tribological performance of silver nanoparticle-enhanced polyethylene glycol lubricants. Tribol Trans 59:585–592
[12] Amorim PM, Ferraria AM, Colaço R, Branco LC, Saramago B (2017) Imidazolium-based ionic liquids used as additives in the nanolubrication of silicon surfaces. Beilstein J Nanotechnol 8:1961–1971
[13] Li YQ, Wang QH, Wang TM, Pan GQ (2012) Preparation and tribological properties of graphene oxide/nitrile rubber nanocomposites. J Mater Sci 47:730–738. https://doi.org/10.1007/s10853-011-5846-4
[14] Wang BG, Tang WW, Lu HS, Huang ZY (2016) Ionic liquid capped carbon dots as a high-performance friction-reducing and antiwear additive for poly(ethylene glycol). J Mater Chem A 4:7257–7265
[15] Yao MH, Liang YM, Xia YQ, Zhou F (2009) Bisimidazolium ionic liquids as the high-performance antiwear additives in poly(ethylene glycol) for steel-steel contacts. ACS Appl Mater Inter 1:467–471
[16] Cao ZF, Xia YQ (2017) Corrosion resistance and tribological characteristics of polyaniline as lubricating additive in grease. J Tribol-T ASME 139:061801. https://doi.org/10.1115/1.4036271
[17] Gao HX, Jian T, Han BX, Wang Y, Du JM, Liu ZM, Zhang JL (2004) Aqueous/ionic liquid interfacial polymerization for preparing polyaniline nanoparticles. Polymer 45:3017–3019
[18] Athawale AA, Kulkarni MV, Chabukswar VV (2002) Studies on chemically synthesized soluble acrylic acid doped polyaniline. Mater Chem Phys 73:106–110
[19] Wang CC, Song JF, Bao HM, Shen QD, Yang CZ (2010) Enhancement of electrical properties of ferroelectric polymers by polyaniline nanofibers with controllable conductivities. Adv Funct Mater 18:1299–1306
[20] Saini P, Choudhary V (2013) Structural details, electrical properties, and electromagnetic interference shielding response of processable copolymers of aniline. J Mater Sci 48:797–804. https://doi.org/10.1007/s10853-012-6797-0
[21] Tan JL, Xie Z, Zhang Z, Sun YN, Shi W, Ge DT (2018) Dopamine modified polyaniline with improved adhesion, dispersibility, and biocompatibility. J Mater Sci 53:447–455. https://doi.org/10.1007/s10853-017-1520-9
[22] And STH, Okello M (2005) The 2-position of imidazolium ionic liquids: substitution and exchange. J Org Chem 70:1915–1918
[23] Stejskal J, Dybal J, Trchová M (2014) The material combining conducting polymer and ionic liquid: hydrogen bonding interactions between polyaniline and imidazolium salt. Synth Met 197:168–174
[24] Pramanik S, Karak N, Banerjee S, Kumar A (2012) Effects of solvent interactions on the structure and properties of prepared PAni nanofibers. J Appl Polym Sci 126:830–836
[25] Li R, Chen Z, Li J, Guo Q (2013) Effective synthesis to control the growth of polyaniline nanofibers by interfacial polymerization. Synth Met 171:39–44
[26] Fan XQ, Wang LP (2015) Ionic liquids gels with in situ modified multiwall carbon nanotubes towards high-performance lubricants. Tribol Int 88:179–188
[27] Leng C, Wei J, Liu Z, Shi J (2011) Influence of imidazolium-based ionic liquids on the performance of polyaniline-CoFe2O4 nanocomposites. J Alloys Compd 509:3052–3056
[28] Battez AH, González R, Viesca JL, Blanco D, Asedegbega E, Osorio A (2009) Tribological behaviour of two imidazolium ionic liquids as lubricant additives for steel/steel contacts. Wear 266:1224–1228
[29] Cai MR, Liang YM, Yao MH, Xia YQ, Zhou F, Liu WM (2010) Imidazolium ionic liquids as antiwear and antioxidant additive in poly(ethylene glycol) for steel/steel contacts. ACS Appl Mater Inter 2:870–876
[30] Minami I (2009) Ionic liquids in tribology. Molecules 14:2286–2305
[31] Jiménez AE, Bermúdez MD, Iglesias P, Carrion FJ, Martinez-Nicolas G (2006) 1-*N*-alkyl-3-methylimidazolium ionic liquids as neat lubricants and lubricant additives in steel-aluminium contacts. Wear 260:766–782
[32] Anand M, Hadfield M, Viesca JL, Thomas B, Battez AH, Austen S (2015) Ionic liquids as tribological performance improving additive for in-service and used fully-formulated diesel engine lubricants. Wear 334–335:67–74
[33] Nunn N, Mahbooba Z, Ivanov MG, Ivanov DM, Brenner DW, Shenderova O (2015) Tribological properties of polyalphaolefin oil modified with nanocarbon additives. Diamond Relat Mater 54:97–102
[34] Padgurskas J, Rukuiza R, Prosyčevas I, Kreivaitis R (2013) Tribological properties of lubricant additives of Fe, Cu and Co nanoparticles. Tribol Int 60:224–232
[35] Ge XY, Xia YQ, Cao ZF (2015) Tribological properties and insulation effect of nanometer TiO_2 and nanometer SiO_2 as additives in grease. Tribol Int 92:454–461

[36] Fan XQ, Li W, Fu HM, Zhu MH, Wang LP, Cai ZB, Liu JH, Li H (2017) Probing the function of solid nanoparticle structure under boundary lubrication. ACS Sustain Chem Eng 5:4223–4233

[37] Liu Y, Zhang XF, Dong SL, Ye ZY, Wei YD (2017) Synthesis and tribological property of Ti_3 C_2T_X nanosheets. J Mater Sci 52:2200–2209. https://doi.org/10.1007/s10853-016-0509-0